Electronic Supplementary Material (ESI) for Lab on a Chip.

Supporting Information

Acoustofluidics-based microscopic examination for automated and point-of-care urinalysis

Xin He[‡ ab] *Feng Ren,*[‡ c] *Yangyang Wang,*[ab] *Zhiyuan Zhang,*[ab] *Jiming Zhou,*[ab] *Jian Huang,*[ab] *Shuye Cao,*[ab] *Jinying Dong,*[c] *Renxin Wang,*[d] *Mengxi Wu*[*ab] *and Junshan Liu*[*ab]

*Corresponding author. Email: mengxiwu@dlut.edu.cn (M. Wu), liujs@dlut.edu.cn (J. Liu)

This file includes:

Note S1. Numerical simulation

The microfluidic chip was simulated using COMSOL Multiphysics to investigate the fluidic and acoustic field in the channel as well as the behavior of micron-size particles in acoustofluidics. In this study, the 2D simulation of the microfluidic device was divided into three modules/steps, i.e., steady-state flow field simulation, acoustic field simulation and particle trajectory simulation. To save computational resources and time, the mesh size was decreased at the straight channel and progressively increased in each trident branch.

The steady-state flow field simulation was utilized to analyze the flow state of liquid in the channel. The flow rate on the inlet was set at 1 mL·min-1 and the outlets were imposed as the open end (0 Pa) condition as the boundary condition of the flow field simulation. Reynold's number was low in the experiment thus the stationary incompressible Navier-Stokes was adopted in the simulation.

The pressure acoustic module was used to analyze the acoustic field in the channel. Since the microparticles used in the present study were large enough to ignore the acoustic streaming force, only the acoustic radiation force (ARF) was considered. An acoustic pressure at the frequency of 2.001MHz was applied to one side of the long straight wall of the main channel. The acoustic wave propagated from this wall and was reflected by the other hard channel wall. There was a straight acoustic pressure node line in the middle of the straight channel, which was formed by the resonance of standing acoustic waves reflected by hard channel walls. The liquid-silicon and liquid-air boundaries were set as sound hard (impedance) boundary and sound soft boundary.

The particle tracing module was used to analyze the trajectory of particles inside the channel. For this part of the simulation, 200 particles were released at time zero second and distributed homogenously. Then, the ARF and the drag force induced by liquid flowing were applied to the particles, The values of the applied parameters were the same as that in previous sections.

Note S2. Design and fabrication of the microchip

The fabrication process of the microchip is shown in the Figure S3. The microchannel was manufactured on the silicon wafer using deep reactive ion etching (PSE V300, NAURA, China), and then the silicon wafer was sealed with a BF33 glass wafer by anodic bonding (850LT, EVG, China). After that, the chip was cut by a scribing machine (8230, ATMI, China) with the inlet and outlet of the channel exposed. It cooperates with silicon tubes through the holder as shown in the Figure 2. A PZT transducer (RP150, Murata, Japan) with the resonant frequency of 2MHz was glued underneath the chip using cyanoacrylate glue (Scotch weld, Seatac, China) and actuated using a function generator (DG1062, RIGOL, China) coupled to an amplifier (ATA-3040, Aigtek, China). The size of PZT transducer was 20mm x 20mm x 1mm. The temperature is monitored *via* a PT100 temperature sensor (CRZ-1632, HAYASHI, Japan) attached to the bottom of the chip. The temperature is controlled to be less than 37°C by the fan and the heat dissipation of the holder.

Note S3. Design and fabrication of the holder

The holder was used for the interconnection of the acoustofluidics-based chip and the pumps. It was designed using the 3D-printing technology and comprised by two pedestals, which corresponds to the inlet and outlet of the chip. There are two elastic gaskets between the chip and the holders that can prevent the leakage of liquid. And there are corresponding channels in pedestals and gaskets. The pedestals, elastic gaskets and chip are clamped by four bolts and form a continuous flow path. Short silicon tubes can be connected to the holder conveniently from both sides which can not only avoid the interference between the tubes and the microscope objective but also can avoid the block of channel by glue which was used for the connection of chips and silicon tubes.

The outlet of the holder aligns accurately to the micro dispensing module. As shown in the Figure 6A and S4, the disposable micro dispensing module is constituted by the bottom glass slide, the coverslip glass and two PDMS films (DC80, Westru, China). The PDMS films are attached to the bottom slide glass and coverslip based on the Van der Waals force thus a semi-closed chamber was formed.

Note S4. Experimental Setup

Polystyrene microspheres (Thermo Fisher Scientific) with diameter of 10μm and 15μm with an initial solids content of 1% were diluted with deionized water with a particle concentration of 1×10^4 counts per mL to evaluate the concentration performance. The cell distribution across the channel was observed using a microscope (MF43-N, Mshot, China) and captured using a CCD camera (AcutEye-1M, Ketianjian, China) attached to the microscope. The captured image frames were processed using the ImageJ software (https:// imagej.nih.gov/ij/) to create composite images to illustrate the acoustic focusing behaviors. Sodium fluorescein (S353, Boer, China) was diluted with DI water to 1g/L to show the flow streamline of liquid in this work.

Note S5. Patient's Urine Acquisition

Urine samples were collected from patients taking part in the medical examination in the Second Hospital of Dalian Medical University. Fifty randomly selected patients who attended the laboratory of the hospital were studied and at least 15 mL urine were collected for each person. All experiments were performed in compliance with the Chinese laws and followed the institutional guidelines. This study was approved by the Institutional Ethical Committee for Clinical Research for The Second Hospital of Dalian Medical University, and the urine were collected after the approval of the patients. The collected urine was stored in sterile glass bottles and used within 2 hours of collection.

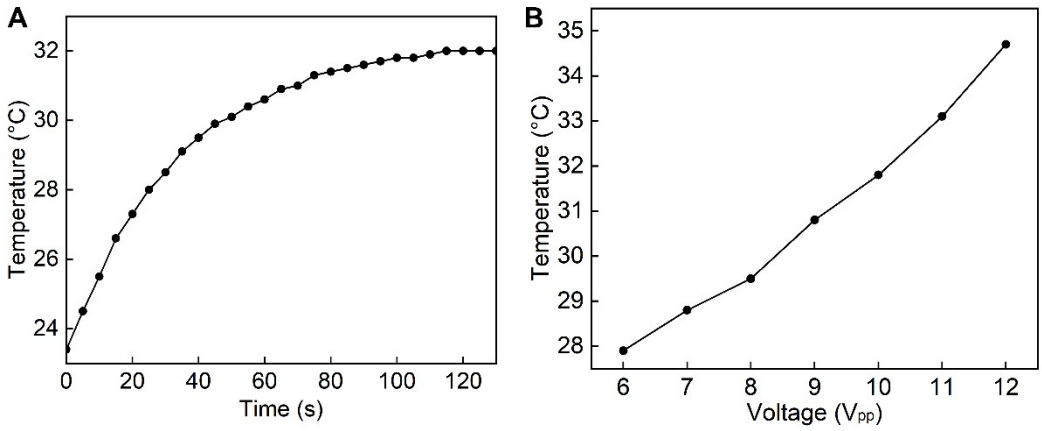

Figure S1. Thermal characterization. A) The temperature of the chip with cooling detected by the sensor in 130s. The PZT transducer is driven at 10 V and the flow rate is 1000 μL·min^{-1}. B) The temperature of the chip at different actuation voltage from 6 V to 12 V. The temperature was measured 3 minutes after operating.

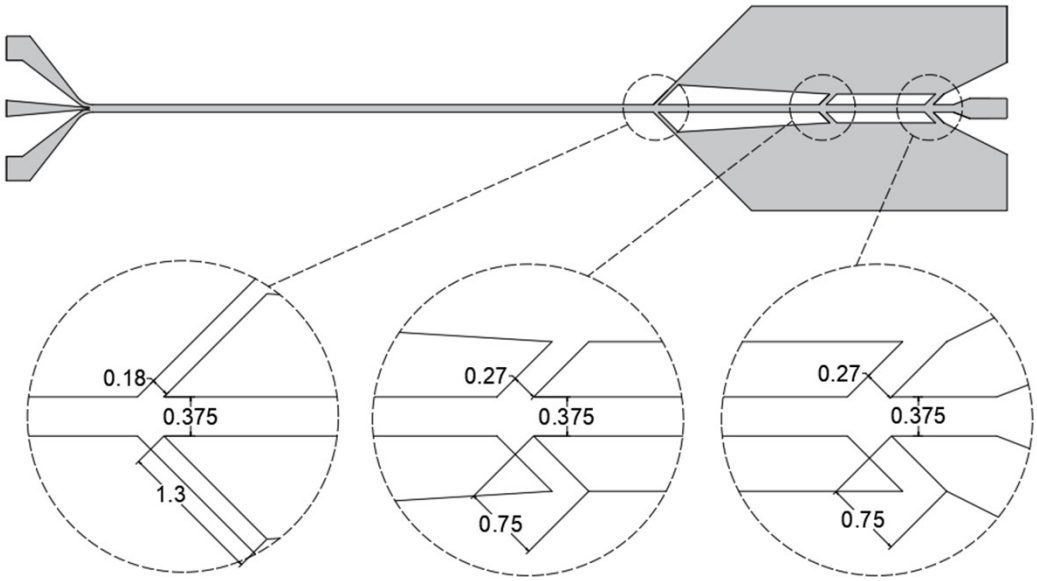

Figure S2. The structure and size of the microchip (unit:μm).

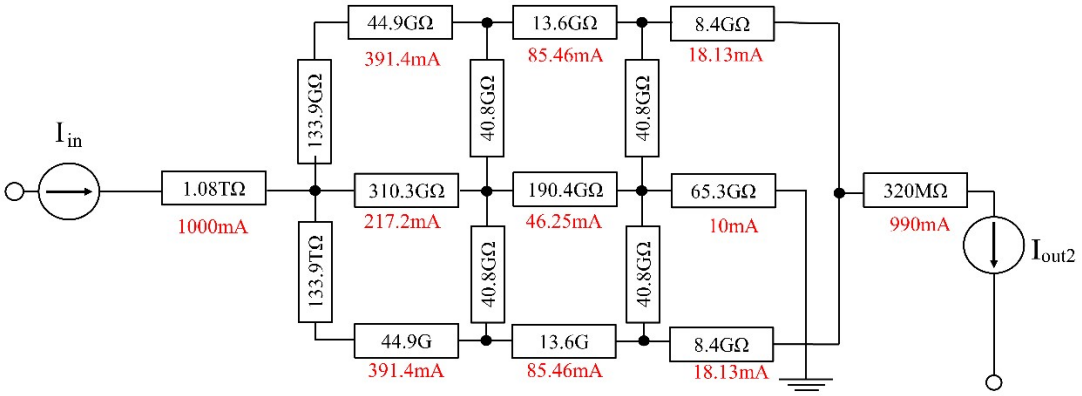

Figure S3. Electric circuit simulation based on the hydraulic-electric analogy.

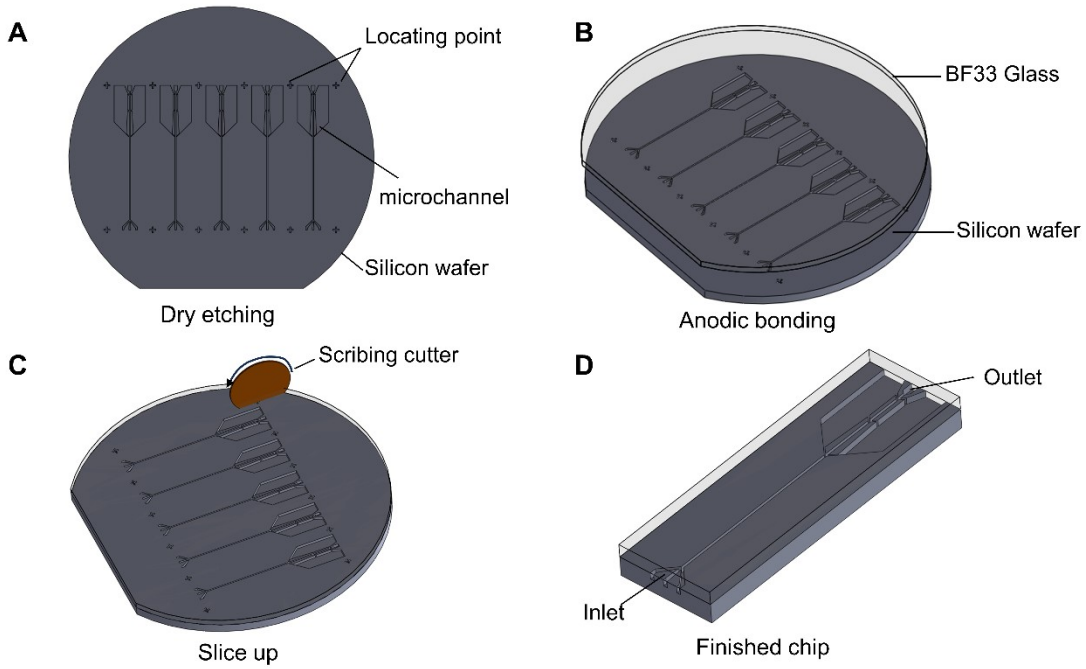

Figure S4. Fabrication process of the microchip. The microchannel is manufactured on the silicon wafer using deep reactive ion etching, and is sealed by anodic bonding of a glass lid. Then the chip is cut by a scribing machine with the inlet and outlet of the channel exposed to the side directions.

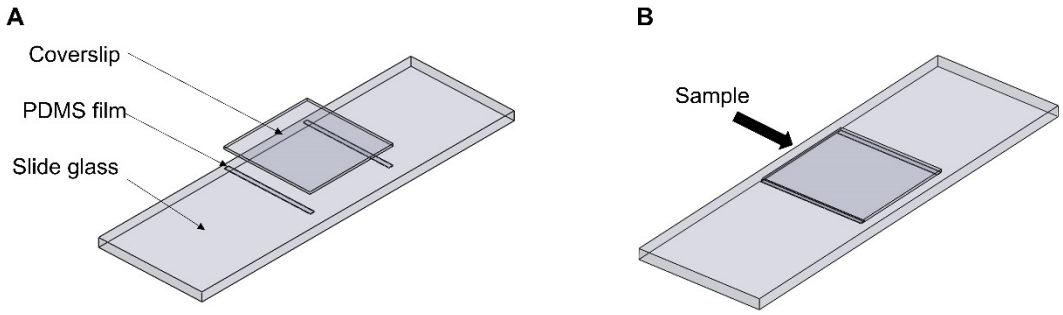

Figure S5. Fabrication process of the disposable micro dispensing module. The microdevice are constituted by the bottom glass slide, the coverslip glass (15×15 mm) and two PDMS films. The PDMS films are attached to the glass based on the Van der Waals force and a semi-closed chamber is formed.

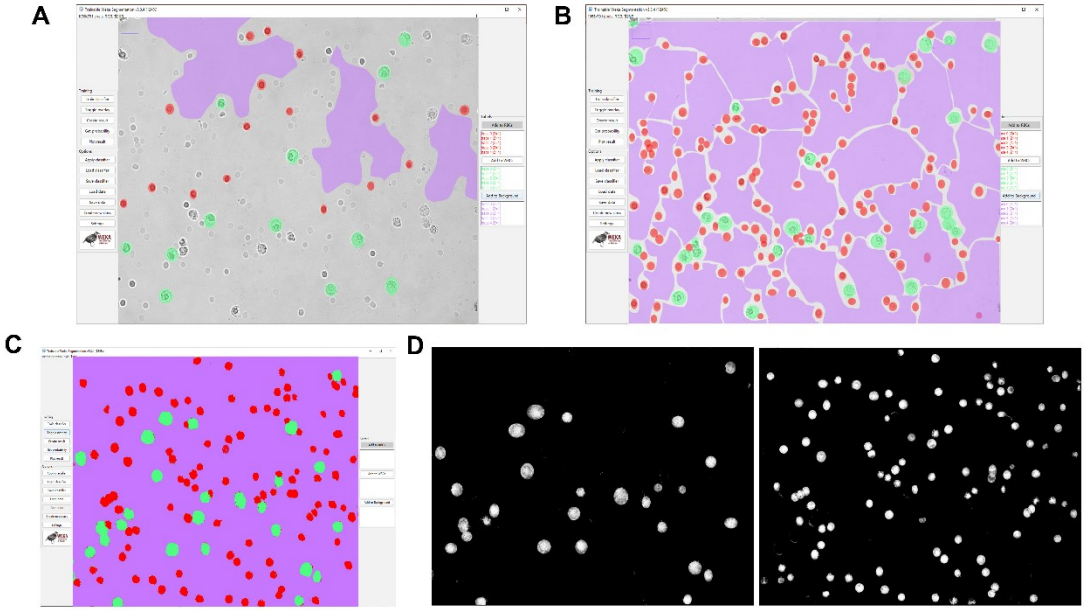

Figure S6. The training process of the machine learning classifier. A) RBCs and WBCs in the training set are distinguished and marked by two experienced medical technologists. B) Then the classifier can be trained to learn from the input marked training data and C) perform later in unknown images to detect and segment between RBCs and WBCs. D) After being separated by the classifier, RBCs and WBCs are quantitively analyzed independently.

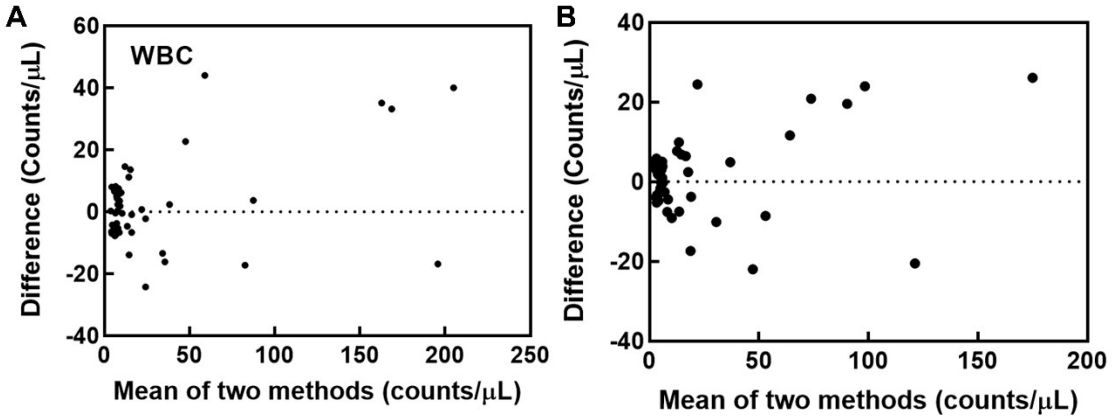

Figure S7. The comparison of acoustofluidics-based system and manual microscopy method for urine test of fifty samples. Bland–Altman analysis of cell counting result for A) WBC and B) RBC using this system and manual microscopy method. The X-axis of these figures shows the mean of these two methods and Y-axis shows the value that the manual microscopy method minus that of this system.

Manual microscopy										
Particles	WBCs (Cells/HPF)	0-5	6-10	11-20	>20	RBCs (Cells/HPF)	0-5	6-10	11-20	>20
Acoustofluidic method	0-5	26	4	1	0	0-5	29	2	1	0
	6-10	2	3	1	0	6-10	3	4	0	0
	11-20	1	0	5	1	11-20	1	0	2	0
	>20	0	0	0	6	>20	0	0	1	7
	Concordance rate	80%				Concordance rate	84%			
	Concordance rate within ± 1 grading	96%				Concordance rate within ± 1 grading	96%			

Figure S8. The comparison of acoustofluidics-based system and manual microscopy method for urine test of fifty samples. The cell densities are converted to the same scales before data analysis. The results are divided into four grades (0-5, 6-10, 11-20 and above 20). The gray-shaded areas represent the number of cases within the same grade and the blue-shaded areas represent the number of cases within one grade difference.

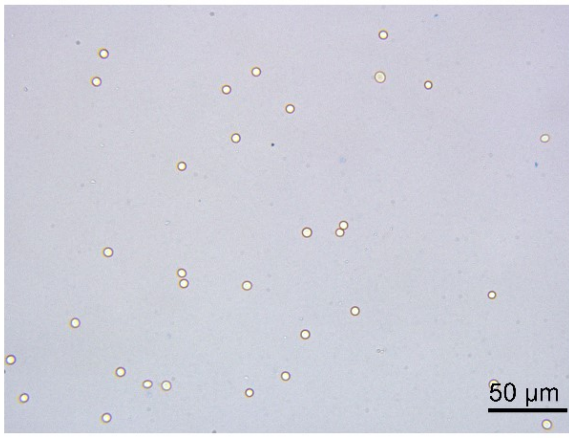

Figure S9. Biocompatibility characterization. The microscopic image of the sample processed by the chip at 10.2V voltage and stained with 0.4% Trypan Blue reagent solution.

Shape	Rectangular(w×h)					Circular (d)
Dimension [μm]	4500×100	1000×100	375×100	270×100	180×100	2
R [$\times 10^{12}$·Pa·s·m^{-4}]	2.69	12.8	38.7	58.4	103.0	0.0025

Table S1. Hydraulic resistances in a unit length.

		R1	R2	R2'	R2''	R3	R3'	R3''	R4	R4'	R4''	R5
R [$\times 10^9$·Pa·s·m^{-4}]		1086.0	310.3	133.9	44.9	190.4	40.8	13.6	190.4	40.8	8.4	0.32
Dimensions [mm]	4.2×0.1	-	-	-	7.5	-	-	5	-	0.75	3.1	-
	1×0.1	-	-	-	-	-	-	-	1.5	-	-	-
	0.375×0.1	28	8	-	-	5	-	-	1	-	-	-
	0.27×0.1	-	-	-	-	-	0.75	-	-	-	-	-
	0.18×0.1	-	-	1.3	-	-	-	-	-	-	-	-

Table S2. Hydraulic resistances of each channel.